Modelling the phase equilibria and excess properties of the water + carbon dioxide binary mixture

María Carolina dos Ramos* and Felipe J. Blas†
Departamento de Física Aplicada,
Facultad de Ciencias Experimentales,
Universidad de Huelva, 21071 Huelva, Spain

Amparo Galindo‡
Department of Chemical Engineering,
Imperial College London, South Kensington Campus,
London SW7 2AZ, United Kingdom

The high-pressure phase diagram and excess thermodynamic properties of the binary mixture of carbon dioxide and water are examined using the statistical associating fluid theory for potentials of variable range (SAFT-VR). The carbon dioxide molecule is modelled with two tangentially bonded spherical segments, while the water molecule is modelled as spherical with four associating sites to represent the hydrogen bonding. Dispersion interactions are modelled using square-well potentials. The optimised intermolecular parameters are taken from the works of Galindo and Blas [*Fluid Phase Equil.* **194-197**, 501 (2002); *J. Phys. Chem. B* **106**, 4503 (2002)] and Clark *et al.* [*Mol. Phys.* **22-24**, 3561 (2006)] for carbon dioxide and water, respectively. The mixture exhibits type III phase behaviour in the classification of Scott and van Konynenburg, with the gas-liquid critical line continuously changing into a liquid-liquid line at high pressures. In this work one unlike intermolecular interaction parameter is fitted to give the best possible representation of the minimum temperature of the gas-liquid critical line of the mixture, and is then used in a transferable manner to study other thermodynamic conditions and properties. The phase diagrams predicted by the SAFT-VR approach are found to be in very good agreement with the experimental data at low and high pressures and temperatures. In addition, a good qualitative description of the excess molar volume and excess enthalpy and different temperatures and pressures is obtained.

I. INTRODUCTION

In recent years the use of supercritical carbon dioxide (CO_2) has achieved a great importance in the chemical industries. Supercritical carbon dioxide is being considered as a substitute solvent of conventional organic solvents, which are often associated to health and environmental concerns [1]. By comparison, CO_2 is relatively non-toxic, non flammable, relatively inert in most processes, very inexpensive (and hence economically profitable) and nonpolluting, it has a greater solvation power, is readily recovered and recycled. There are numerous areas in which processes are using CO_2 as a solvent, including separations in the food industry, coatings, polymer production and dry-cleaning [2]. Other applications and uses of CO_2 are of interest within the oil and gas industries. For instance, in enhanced oil recovery where it is injected it in order to extract more crude. In the context of geochemistry and environmental technology, particularly, due to the increasing concern to reduce the amount of carbon dioxide in the atmosphere CO_2 capture and storage is under much examination. For example, the storage of carbon dioxide by means of sequestration into depleted hydrocarbon reservoirs, by injecting into saline aquifers or by using the industrial fixation into inorganic carbonate is being considered [3–5]. In addition, the presence of both carbon dioxide and water in such environments can lead to the formation of hydrates, a problem of crucial interest to the oil industries in itself.

Carbon dioxide and water mixtures exhibit large regions of liquid-liquid separation, and from an experimental point of view, most of the interest has focused on the mutual solubilities. This research has produced a large amount of experimental data. We recommend the excellent reviews of Larryn and Akinfiev [6], Spycher *et al.* [7] and Chapoy *et al.* [8] for additional information. More recently, Valtz *et al.* [9] have studied in detail the vapour-liquid (VL) equilibria

*Current address: Department of Chemical Engineering, Vanderbilt University, Nashville, TN 37235 (USA); Electronic address: maria.dosramos@vanderbilt.edu
†Corresponding author; Electronic address: felipe@uhu.es
‡Electronic address: a.galindo@imperial.ac.uk

of the mixture. From a theoretical point of view, the water + carbon dioxide binary mixture exhibits type III phase behaviour according to the Scott and van Konynenburg classification [10, 11], with characteristic extensive liquid-liquid immiscibility. The gas-liquid critical line starting at the critical point of the less volative component (water in this mixture) continues to high-pressures turning into a so-called fluid-fluid critical line, or sometimes denoted as gas-gas (GG) immiscibility of second kind. In systems that exhibit this kind of immiscibility, the critical line that departs from the less volatile component has a negative slope as the pressure increases, passing through a temperature minimum, then developing a positive slope at higher pressures. In the low-pressure region, liquid-liquid-vapour three-phase coexistence is observed, and a three-phase line extends from low pressures and temperatures to an upper critical end point (UCEP) found close to the critical point of the more volatile component (CO_2). A short gas-liquid critical line is seen between the UCEP and the gas-liquid critical point of the volatile component. A further interesting feature of the water + carbon dioxide binary mixture is that it presents barotropic inversion, i.e., an inversion of the density due to a pressure effect [12]. Theoretical studies have mainly been concerned with the solubilities [13], hydrate formation [14], and vapour-liquid phase behaviour in small ranges of temperature and pressure [9]. Despite the large amount of studies dealing the water + carbon dioxide binary mixture, there are few describing its global phase behaviour and other thermodynamic properties [9, 13–15]. Here we use the molecular-based statistical associating fluid theory for potentials of variable range (SAFT-VR) [16, 17] to carry out such a study. The approach has proven very useful in previous studies involving complex fluids in general [18], and in particular CO_2 [19, 20] and H_2O [21, 22].

We use the SAFT-VR approach to examine the pressure-temperature phase diagram of the mixture for a wide range of conditions, from the high-pressure critical region to the low-pressure three-phase region. In addition we test the proposed model by comparing calculated excess thermodynamic functions with experimental data available in the literature. Although analytical equations of state such as SAFT-VR cannot provide an accurate description of the critical region as well as of the phase behaviour far away from critical points, it is possible through re-scaling the pure component parameters, and by fitting the unlike intermolecular interaction parameters to critical data, to provide accurate descriptions of the global pressure-temperature PT phase diagrams of mixtures. We have followed this procedure in previous works to study the phase behaviour of CO_2 + n-alkane mixtures and were able to reproduce transitions in type of phase behaviour for increasing carbon number [19, 20]. In this work we pursue a similar goal; i.e., to reproduce the overall PT phase diagram for a binary mixture of carbon dioxide and water. We have hence, fitted one unlike interaction mixture parameter to the temperature minimum of the fluid-fluid critical line of the mixture. Once the unlike parameter is determined, we study the phase behaviour at other conditions of pressure and temperature, as well as other thermodynamic properties. In particular, we investigate the global phase behaviour of the binary mixture. The ability of the theoretical approach to predict different thermodynamic properties is also tested by comparing calculated excess volume and enthalpy of the mixture with corresponding experimental data. This is a stringent test since excess thermodynamic functions are very sensitive to the molecular details of a model.

The rest of the paper is organised as follows: the molecular model and theory are described in section II, where we also highlight the most relevant features of the molecular parameters used in this work; results and discussion are presented in section III; and conclusions are given in section IV.

II. MOLECULAR MODEL AND THEORY

Water molecules are modelled as spherical using the four-site model proposed by Bol [23] and Nezbeda *et al.* [24]. In this model the molecules are represented as hard-spheres of diameter σ_{11}, with four off-centre short-range attractive sites, which mediate the hydrogen bonding interactions. Two of the sites (of type H) represent the hydrogen atoms in the water molecule and the other two sites (of type O) represent the lone pairs of electrons of the oxygen. Only H–O site-site interactions are allowed, i.e., no H–H or O–O interactions are allowed. The associating sites are placed at a distance r_d from the centre of the sphere and have a cut off range of r_c, so that when the site-site distance is less than r_c a hydrogen-bonding energy of interaction ϵ_{hb} is realised. Very recently, Clark *et al.* [21] have revisited the determination of optimal intermolecular parameters for this model. See this work and reference therein for further details.

Following earlier work [19, 20], carbon dioxide molecules are modelled with a simple united atom approach, in which m_2 hard-sphere segments of equal diameter σ_{22} are bonded tangentially. It is important to mention that the polar and quadrupolar interactions of water and carbon dioxide are treated in an effective way via the square-well interactions of variable range. The square-well interaction between segments i and j separated by a distance r is given by:

$$u_{ij}(r) = \begin{cases} +\infty & \text{if } r < \sigma_{ij} \\ -\epsilon_{ij} & \text{if } \sigma_{ij} \leq r \leq \lambda_{ij}\sigma_{ij} \\ 0 & \text{if } r > \lambda_{ij}\sigma_{ij} \end{cases} \tag{1}$$

where σ_{ij} defines the contact distance between spheres, and λ_{ij} and ϵ_{ij} are the range and depth of the potential well for the *i*-*j* interaction, respectively.

In our model we do not incorporate CO_2-CO_2 association interactions or cross-association interactions between CO_2 and H_2O molecules, although we note that other authors have discussed this possibility. Valtz *et al.* [9] suggested that the unusual large interaction parameters they find for this mixture may be an indication of the need to incorporate a cross-association scheme for this mixture. They considered a model for CO_2 incorporating association sites, but on fitting to experimental data the optimal bonding energy was found to be of a value close to zero, and they rejected the idea. More recently, Ji *et al.* [15] have modelled carbon dioxide as an associating molecule with three sites that model the self-association in the CO_2 and the association of CO_2 and H_2O molecules due to the quadrupolar moment.

We use the SAFT-VR approach to study the phase behaviour and excess properties of the mixture. Since the theory has already been presented [16, 17], we provide only a brief overview of the main expressions. The SAFT-VR equation is written in terms of the Helmholtz free energy, expressed as the sum of four microscopic contributions: an ideal contribution A^{IDEAL}, a monomer term A^{MONO}, which takes into account the attractive and repulsive forces between the segments that form the molecules, a chain contribution A^{CHAIN}, which accounts for the connectivity of the molecules, and an association term A^{ASSOC}, which takes into account intermolecular association. The free energy is then written as:

$$\frac{A}{Nk_{\mathrm{B}}T} = \frac{A^{\mathrm{IDEAL}}}{Nk_{\mathrm{B}}T} + \frac{A^{\mathrm{MONO}}}{Nk_{\mathrm{B}}T} + \frac{A^{\mathrm{CHAIN}}}{Nk_{\mathrm{B}}T} + \frac{A^{\mathrm{ASSOC}}}{Nk_{\mathrm{B}}T}, \tag{2}$$

where N is the total number of molecules, T is the temperature, and k_{B} is the Boltzmann constant.

The free energy of the ideal mixture is given by [25]:

$$\frac{A^{\mathrm{IDEAL}}}{Nk_BT} = \sum_{i=1}^{n} x_i \ln(\rho_i \Lambda_i^3) - 1, \tag{3}$$

where $\rho_i = N_i/V$ is the number density, x_i the molar fraction, and Λ_i is the thermal de Broglie wavelength of species i.

The monomer free energy is written as a second-order high temperature perturbation expansion [26–28]:

$$\frac{A^{\mathrm{MONO}}}{Nk_BT} = \frac{A^{\mathrm{HS}}}{Nk_BT} + \frac{A_1}{Nk_BT} + \frac{A_2}{Nk_BT}, \tag{4}$$

A^{HS}/Nk_BT is the residual free energy of a mixture of hard spheres, and A_1/Nk_BT and A_2/Nk_BT are the first- and second-order perturbation terms associated with the attractive interactions $u_{ij}(r)$ given by Eq. (1). The residual free energy of the reference hard-sphere mixture is obtained from the expression of Boublík [29] (equivalent to that of Mansoori *et al.* [30]), the mean-attractive energy associated with the first-order perturbation term is treated in the context of the M1Xb mixing rule [17] and the second-order perturbation term is obtained using the local compressibility approximation.

The contribution to the free energy due to the formation of chains of square-well segments can be written as [17, 31, 32]:

$$\frac{A^{\mathrm{CHAIN}}}{Nk_{\mathrm{B}}T} = -\sum_{i=1}^{n} x_i(m_i - 1)\ln y_{ii}^{\mathrm{SW}}(\sigma_{ii}) = -x_2(m_2 - 1)\ln y_{22}^{\mathrm{SW}}(\sigma_{22}), \tag{5}$$

where m_i is the number of segments of component i, $y_{ii}^{\mathrm{SW}}(\sigma_{ii}) = g_{ii}^{\mathrm{SW}}(\sigma_{ii})\mathrm{e}^{-\beta\epsilon_{ij}}$. The contact pair radial distribution function for a mixture of square-well molecules corresponding to the $i-i$ interaction, $g_{ii}^{\mathrm{SW}}(\sigma_{ii})$, is obtained from a high-temperature expansion [26–28] to first order (see [16, 17] for further details).

The contribution to the free energy due to the association of s_i sites on a molecule of species i can be obtained from the theory of Wertheim [33–36] as:

$$\frac{A^{\mathrm{ASSOC}}}{Nk_BT} = \sum_{i=1}^{n} x_i \left[\sum_{a=1}^{s_i}\left(\ln X_{a,i} - \frac{X_{a,i}}{2}\right) + \frac{s_i}{2}\right] = x_1\left[4\left(\ln X - \frac{X}{2}\right) + 2\right], \tag{6}$$

where the first sum is over species i and the second over all s_i sites of type a on a molecule i. Since there is only one type of hydrogen bond for the water molecule, the fractions X of water molecules not bonded at any of the four sites are equivalent. This, together with the absence of water-carbon dioxide association greatly simplifies the analysis. The fraction $X_{a,i}$ of molecules i not bonded at site a is given by the mass action equation as [37, 38]:

$$X_{a,i} = \frac{1}{1 + \sum_{j=1}^{n} \sum_{b=1}^{s_j} \rho x_j X_{b,j} \Delta_{a,b,i,j}} = X = \frac{1}{1 + 2\rho x_1 \Delta}, \tag{7}$$

where $\Delta_{a,b,i,j}$ characterizes the association between site a on molecule i and site b on molecule j. It can be written as [16, 17]:

$$\Delta_{a,b,i,j} = K_{a,b,i,j} F_{a,b,i,j} g_{ij}^{\mathrm{SW}}(\sigma_{ij}) = \Delta = K_{11} F_{11} g_{11}^{\mathrm{SW}}(\sigma_{11}), \tag{8}$$

where the Mayer f-function of the $a-b$ site-site interaction $\phi_{a,b,i,j}$ is given by $F_{a,b,i,j} = \exp(-\phi_{a,b,i,j}/k_B T) - 1$, and $K_{a,b,i,j}$ is the available volume for bonding. Since in the mixture there is only one type of water-water hydrogen bond, the only subscripts remaining indicate that the only association is between molecules of component 1 (water). The corresponding Mayer f-function is then given by $F = \exp(\epsilon_{11}^{\mathrm{HB}}/k_{\mathrm{B}}T) - 1$. The expression for the bonding volume can be found elsewhere [16, 17, 37].

Other thermodynamic properties, such as the chemical potential μ, compressibility factor Z, and other thermodynamic derivatives needed in our calculations can be easily obtained from the Helmholtz free energy using standard thermodynamic relations.

III. RESULTS

In order to treat real compounds the intermolecular model parameters need to be determined. In the case of water these are: the number of segments forming the model molecule, $m_1 = 1$ (since is treated as spherical), the segment hard-core diameter σ_{11}, depth ϵ_{11} and range λ_{11} of the square-well interaction, and two additional parameters to characterise the site-site interactions, the hydrogen bonding energy ϵ^{HB}, and available volume K^{HB}. The complete set of parameter values are taken from the recent work of Clark *et al.* [21], and are also presented in Table I. Similarly, carbon dioxide, which is modelled as non-associating, is described by means of four molecular parameters: the number of segments forming the model molecule, $m_2 = 2$, the segment hard-core diameter σ_{22}, and the depth ϵ_{22} and range λ_{22} of the square-well interaction. In this work we use the parameter values obtained by Blas and Galindo [19] (see also in Table I). Both sets of parameters are able to provide a very good description of the vapor pressures and coexistence densities for a wide range of temperatures (see our previous works for further details [19–21]) with the exception of the critical region. This is an expected behavior since SAFT-VR, as any classical equation of state, does not consider the density fluctuations that occur near the critical point. However, since we have an interest in the high-pressure phase equilibria and critical behavior of the H_2O + CO_2 binary mixture, we have rescaled the conformal parameters (σ_c and ϵ_c) to the experimental critical temperature and pressure. The rescaled parameters are also presented in Table I. The remaining, non-conformal parameters, are kept fixed in reduced units, their corresponding values in real units are also presented in the table for clarity. Throughout this work the parameters scaled to the critical points are used.

The calculation of mixture properties also requires to determine several unlike intermolecular parameters. In our case, σ_{12} is given by the arithmetic mean, $\sigma_{12} = (\sigma_{11} + \sigma_{22})/2$, and $\lambda_{12} = (\lambda_{11}\sigma_{11} + \lambda_{22}\sigma_{22})/(\sigma_{11} + \sigma_{22})$. The unlike dispersive energy is written as $\epsilon_{12} = \xi_{12}\sqrt{\epsilon_{11}\epsilon_{22}}$, with $\xi_{12} = 0.9742$. We have adjusted ξ_{12} to give the best possible representation of the temperature minimum of the fluid-fluid critical line of the mixture. This adjusted unlike parameter is treated as temperature-independent, and used to study the complete pressure-temperature-composition PTx phase behaviour of the mixture in a wide range of conditions. In addition, as we will show later, a number of excess properties are also predicted using these model parameters.

The PT projection of the PTx surface for the H_2O + CO_2 mixture is shown in Fig. 1. As can be seen, the phase behaviour of the system is dominated by large regions of liquid-liquid (LL) immiscibility. The mixture exhibits two separated gas-liquid (GL) critical lines. At high pressures and temperatures a critical line starts from the critical point of pure water (647 K and 22.03 MPa) extending to higher pressures, first with a negative slope, through a temperature minimum (450 K and 190 MPa), and then continuing with a positive slope to higher temperatures and pressures. This distinctive feature of the phase behaviour exhibited by the water + carbon dioxide mixture is an example of the gas-gas immiscibility mentioned in the introduction. At lower temperatures and pressures a much shorter critical line

starts at the critical point of pure carbon dioxide (304.21 K and 7.383 MPa) and ends at slightly higher pressures at UCEP, where the GL region, richer in CO_2, disappears into the region of LL immiscibility. The dashed-line shown in the inset of the figure is the predicted three-phase line that runs from very low temperatures and pressures to the UCEP; it corresponds to pressures and temperatures where the two immiscible liquid phases coexist with a gaseous phase. As can be seen, the theory is able to provide a good description of the whole PT projection of the PTx surface of the phase diagram. It is important to note that only one parameter is necessary in order to describe the phase behaviour for the entire fluid range, including the existence of the temperature minimum in the high-pressure critical line.

Different GL and LL regions of the phase diagram of the mixture become clearer in the constant-temperarature Px slices of the PTx surface shown in Fig. 2. In Fig. 2 (a) a Px slice at 288.15 K, a temperature below the UCEP of the mixture and below the critical point of pure CO_2 is shown. As can be seen, three homogeneous phases (a gas, a CO_2-rich liquid and an H_2O-rich liquid) bound the coexistence envelopes of this slice. At temperatures below the three-phase coexistence, a CO_2-rich gas phase coexists with the H_2O-rich liquid phase, above the three-phase temperature a large region of LL immiscibility is seen, and a small GL coexistence region is also observed (the CO_2-rich gas is in coexistence with the CO_2-rich liquid phase). The theory is able to predict the main features exhibited by the system at these conditions, including the existence of the three-phase coexistence, although it overestimates the coexisting molar fractions in both liquid phases (above the pressure at which the system exhibits three-phase behaviour), and in the gas phase (below the three-phase line). In Fig. 2 (b) a Px slice, at much higher temperature, namely, $T = 348.15$ K is shown. At these conditions, the system is above the UCEP of the mixture and no LLG coexistence exits. The coexistence envelope shows two different characters, GL coexistence at low pressure, and LL phase behaviour at high pressures. The theory predicts qualitatively the shape of the phase envelope as the pressure is increased, although the coexisting compositions are overestimated in all cases. It is also interesting to note how the phase behaviour of the mixture changes from (a) to (b) as the temperature is increased. The shape exhibited by the phase envelope in the CO_2-rich phase (in Fig. 2a) is a reminiscence of the small gas-liquid coexistence region located above the three-phase line of the mixture in the CO_2-rich phase region shown in part (a). This is also related with the existence of gas-gas immiscibility of second kind, which is essential to understand the experimental data for this mixture, which is however, usually presented in the form of mutual solubilities of H_2O in a CO_2-rich gas (or liquid) phase and CO_2 in H_2O-rich liquid phase (see the work of Spycher and references therein for a detailed revision of the experimental data available in the literature). A more in depth discussion of the behaviour of the mutual solubilities of H_2O and CO_2 is given in [39].

It is also useful to investigate the validity of our model in the study of excess properties of the mixture, which is a very stringent test of any theory and molecular model. We consider the excess thermodynamic volume of the mixture at different conditions. Unfortunately, experimental information of the excess volume, and in general volumetric data, of the water + carbon dioxide mixture is scarce. Here we use the SAFT-VR approach to predict the excess volume of the mixture at fixed $T = 673.15$ K, and several pressures ranging from 9.94 up to 24.99 MPa. It is useful to note that the temperature selected is above the critical temperature of pure water, while most of the pressures considered (all except 24.99 MPa) are below the critical pressure of pure water. It is important to mention at this point that we have used the same molecular parameters (see Table I) and the same unlike parameter value $\xi_{12} = 0.9742$ previously used to obtain the phase diagram of the mixture. The theoretical predictions and experimental data taken from the literature are shown in Fig. 3. As can be seen, at $T = 673.15$ K the excess volumes are positive at all pressures considered, with a nearly quadratic shape. Positive excess values are expected since the water + carbon dioxide mixture is highly nonideal due to the specific interactions (extensive hydrogen bonding) between water molecules. The maximum of the excess volume at different pressures is relatively large, and a sharply increase of the excess volumes is observed as the pressure is varied. The shape of the curve is very symmetric at lower pressures, and becomes more asymmetric as the pressure is increased, with the maximum displaced toward mixture compositions rich in water. The highest degree of asymmetry occurs where the maximum values are achieved, at 24.94 MPa, which is very close with the PT conditions of the critical isochore for pure water (~ 29.2 MPa at 673.15 K). As can be seen, the SAFT-VR equation is able to provide a good description of the excess volume of the mixtures. Although quantitative agreement between theory and experiment is not seen, the SAFT-VR approach is able to predict the most important features exhibited by the excess volume of the mixture, including its variation with pressure.

We finally consider another important excess thermodynamic function, namely, the excess enthalpy of the mixture. In particular, we examine the excess enthalpy at a fixed temperature, $T = 573.15$ K, and at several pressures. As in the case of the excess volume, the experimental excess enthalpy data is scarce and it has only been determined in a limited region of the phase diagram. As can be seen in Fig. 4, the excess enthalpy is positive in the whole composition range. This property is seen to exhibit a particular shape, which is related to the the large region of fluid-fluid immiscibility the system exhibits at these conditions. The excess enthalpy is positive in the entire range of compositions and increases in magnitude as the pressure is decreased. For the lowest pressure, $P = 10.4$ MPa, although it is difficult to distinguish it in the figure, there is a change in the slope of the excess enthalpy at molar

fractions close to 1. In addition, there is a sharp turning point at molar compositions of water $x_1 \approx 0.7$, 0.75 and 0.80, which correspond to the compositions at which the liquid phase disappears (at the corresponding pressures). This means that for water molar fractions between $0.988 - 0.996$ and $0.7 - 0.8$ approximately, the system is in the fluid-fluid two-phase region of the phase diagram. Although the theory is seen to slightly underestimate the values of the excess enthalpy at all compositions, and to overestimate the range of compositions at which the water + carbon dioxide mixture exhibits an homogeneous liquid phase, agreement between theoretical predictions and experimental data is very good. The disagreement is essentially due to the overestimation of the coexistence molar fraction of water in the CO_2-rich liquid phase.

IV. CONCLUSIONS

We have studied the thermodynamic properties of the water + carbon dioxide binary mixture using the SAFT-VR equation of state. Water is modelled as spherical, with four association sites to mediate hydrogen bonding. Carbon dioxide is described as a non-associating chain formed by two attractive spherical segments tangentially bonded together. Since we are interested in the global PT phase behaviour of the mixture, including the critical lines, we have used intermolecular parameters re-scaled to the critical points of the pure components. An unlike energy parameter is also adjusted to give the best representation of the minimum temperature of the gas-liquid critical line, and then used in a transferable manner to study other thermodynamic conditions and properties.

The SAFT-VR equation of state, with the parameters proposed here, is used predict the phase behaviour and the excess thermodynamic properties of the mixture. The theory is able to provide a global description of the most important features of the phase diagram of the mixture: type III phase behaviour, GG immiscibility of second kind, VL equilibria at low temperatures and pressures, and LL phase equilibria at high pressures. Theoretical predictions are compared with experimental data taken from the literature. Agreement between theory and experiment is quite good in all cases. The theory is also used to predict the behaviour of the two most important excess thermodynamic properties, the excess volume and the excess enthalpy. We examine the variation of these properties with pressure, at constant temperature, for the entire composition range. The theoretical predictions are compared with experimental data taken from the literature. The SAFT-VR approach is able to provide a good description of these functions, especially in the case of the excess enthalpy, which is in quantitative agreement with the experimental data. Mixtures involving CO_2 are of increasing interest in many areas, we have shown here that simplified models, which do not take into account explicitly the quadrupolar nature of the molecule can nevertheless provide predictive information of crucial thermodynamic properties of these mixtures.

ACKNOWLEDGMENT

M.C.dR. acknowledges the Programme Alβan from the European Union Programme of High Level Scholarships for Latin America (identification number E03D21773VE) for a Fellowship. The authors also acknowledge financial support from project number FIS2004-06627-C02-01 of the Spanish Dirección General de Investigación. Additional support from Universidad de Huelva and Junta de Andalucía is also acknowledged. We also thank Manuel M. Piñeiro and Eduardo J. M. Filipe for useful discussions concerning to the excess enthalpy experimental results.

[1] Kenan Center Web Page., 2006. *http//www2.ncsu.edu/champagne*.
[2] J. M. DeSimone. *Science*, **297**, 799–803, 2002.
[3] IPCC Special Report Carbon Dioxide Capture and Storage, 2005. *http://www.ipcc.ch/index.html*.
[4] CO_2 sequestration, 2002. *http://www.princeton.edu/∼chm333/2002/fall/co_two/intro/*.
[5] The U.S. Department of Energy. Fossyl Energy, 2006. *http://www.fossil.energy.gov/sequestration/*.
[6] L. W. Diamond and N. N. Akinfiev. *Fluid Phase Equil.*, **208**, 265–290, 2003.
[7] N. Spycher, K. Pruess, and J. Ennis-King. *Geochimica et Cosmochimica Acta.*, **67**, 3015–3031, 2003.
[8] A. Chapoy, A. H. Mohammadi, A. Chareton, B. Tohidi, , and D. Richon. *Ind. Eng. Chem. Res.*, **43**, 1794–1802, 2004.
[9] A. Valtz, A. Chapoy, C. Coquelet, P. Paricaud, and D. Richon. *Fluid Phase Equil.*, **226**, 333–344, 2004.
[10] R. L. Scott and P. H. van Konynenburg. *Discuss. Faraday Soc.*, **49**, 87–97, 1970.
[11] P. H. van Konynenburg and R. L. Scott. *Phil. Trans.*, **A298**, 495–540, 1980.
[12] J. S. Rowlinson and F. L. Swinton. *Liquids and Liquid Mixtures*, volume 3rd ed. Butterworth Scientific: London, 1982.
[13] X. Ji, S. P. Tan, H. Adidharma, and M. Radosz. *Ind. Eng. Chem. Res.*, **44**, 7584–7590, 2005.
[14] L. Sun, H. Zhao, S. B. Kiselev, and C. McCabe. *J. Phys. Chem. B*, **109**, 9047–9058, 2005.

[15] X. Ji, S. P. Tan, H. Adidharma, and M. Radosz. *Ind. Eng. Chem. Res.*, **44**, 8419–8427, 2005.
[16] A. Gil-Villegas, A. Galindo, P. J. Whitehead, S. J. Mills, G. Jackson, and A. N. Burgess. *J. Chem. Phys.*, **106**, 4168–4185, 1997.
[17] A. Galindo, L. A. Davies, A. Gil-Villegas, and G. Jackson. *Mol. Phys.*, **93**, 241–252, 1998.
[18] P. Paricuad, A. Galindo, and G. Jackson. *Fluid Phase Equili.*, **194–197**, 87–96, 2002.
[19] F. J. Blas and A. Galindo. *Fluid Phase Equil.*, **194–197**, 501–509, 2002.
[20] A. Galindo and F. J. Blas. *J. Phys. Chem. B*, **106**, 4503–4515, 2002.
[21] G. N. I. Clark, A. J. Haslam, A. Galindo, and G. Jackson. *Mol. Phys.*, **104**, 3561–3581, 2006.
[22] B. H. Patel, P. Paricaud, A. Galindo, and G. C. Maitland. *Ind. Eng. Chem. Res.*, **42**, 3809–3823, 2003.
[23] W. Bol. *Mol. Phys.*, **45**, 605–616, 1982.
[24] I. Nezbeda, J. Kolafa, and Y. V. Kalyuzhnyi. *Mol. Phys.*, **68**, 143–160, 1989.
[25] J. P. Hansen and I. R. McDonald. *Theory of simple liquids*, volume 2nd ed. Academic Press: London, 1990.
[26] J. A. Barker and D. J. Henderson. *J. Chem. Phys.*, **47**, 2856, 1967.
[27] J. A. Barker and D. J. Henderson. *J. Chem. Phys.*, **47**, 4714, 1967.
[28] J. A. Barker and D. J. Henderson. *Rev. Mod. Phys*, **48**, 587–671, 1976.
[29] Tomas Boublík. *J. Chem. Phys.*, **53**, 471–472, 1970.
[30] G. A. Mansoori, N. F. Carnahan, K. E. Starling, T. W. Leland. *J. Chem. Phys.*, **54**, 1523, 1971.
[31] A. Galindo, P. J. Whithead, G. Jackson, and A. N. Burgess. *J. Phys. Chem. B*, **101**, 2082–2091, 1997.
[32] W. G. Chapman. *J. Chem. Phys.*, **93**, 4299–4304, 1990.
[33] M. S. Wertheim. *J. Stat. Phys.*, **35**, 19–34, 1984.
[34] M. S. Wertheim. *J. Stat. Phys.*, **35**, 35–47, 1984.
[35] M. S. Wertheim. *J. Stat. Phys.*, **42**, 459–476, 1986.
[36] M. S. Wertheim. *J. Stat. Phys.*, **42**, 477–492, 1986.
[37] G. Jackson, W. G. Chapman, and K. E. Gubbins. *Mol. Phys.*, **65**, 1–31, 1988.
[38] W. G. Chapman, K. E. Gubbins, G. Jackson, and M. Radosz. *Ind. Eng. Chem. Res.*, **29**, 1709–1721, 1990.
[39] M. C. dos Ramos and F. J. Blas and A. Galindo. *J. Phys. Chem. B.* (in preparation).
[40] A. J. Apelblat. *J. Chem. Thermodynamics*, **31**, 869–893, 1999.
[41] F. Keyes. *J. Mech. Eng. Sci.*, **53**, 132–135, 1931.
[42] I. M. Abdulagatov. *J. Chem. Thermodynamics*, **29**, 1387–1407, 1997.
[43] I. M. Abdulagatov. *J. Chem. Eng. Data*, **43**, 830–838, 1998.
[44] W. J. Gildseth. *J. Chem. Eng. Data*, **17**, 402–409, 1972.
[45] N. S. Osborne. *J. Res. Nat. Bur. Std.*, **10**, 155–188, 1933.
[46] D. R. Douslin. *J. Sci. Instrum.*, **42**, 369, 1965.
[47] A. Egerton. *Philos. Trans. R. Soc. London Ser. A*, **231**, 147, 1932.
[48] L. Besley. *J. Chem. Thermodynamics*, **5**, 397–410, 1973.
[49] C. F. Jenkin and D. R. Pye. *Philos. Trans. R. Soc. London Ser. A*, **213**, 67, 1914.
[50] J. M. Sengers, H. Levelt, and W. T. Chen. *J. Chem. Phys.*, **56**, 595–608, 1972.
[51] C. H. Meyers and M. S. van Dusen. *J. Res. Nat. Bur. Std.*, **10**, 281, 1933.
[52] L. A. Webster and A. J. Kidnay. *J. Chem. Eng. Data*, **46**, 759–764, 2001.
[53] J. G. Harris and K. H. Yung. *J. Phys. Chem.*, **99**, 12021–12024, 1995.
[54] P. Nowak, T. Tielkes, R. Kleinrahm, and W. Wagner. *J. Chem. Thermodynamics*, **29**, 885–889, 1997.
[55] K. Toedheide and E. U. Franck. *Z. Phys. Chem. NF.*, **37**, 387–401, 1963.
[56] S. Takenouchi and G. C. Kennedy. *Am. J. Sci.*, **262**, 1055–1074, 1964.
[57] M. B. King, A. Mubarak, J. D. Kim, and T. R. Bott. *J. Supercrit. Fluids*, **5**, 296–302, 1992.
[58] H. Teng, A. Yamasaki, and M.-K. C. adn H. Lee. *J. Chem. Thermodynamics*, **29**, 1301–1310, 1997.
[59] R. D'Sourza, J. R. Patrick, and A. S. Teja. *Can. J. Chem. Eng*, **66**, 319–323, 1988.
[60] K. Jackson, L. E. Bowman, and J. L. Fulton. *Anal. Chem.*, **67**, 2368–2372, 1995.
[61] P. C. Guillepsie and G. M. Wilson, Vapor-liquid and liquid- liquid equilibria: Water-methane, water-carbon dioxide, water-hydrogen sulfide, water-npentane, water-methane-npentane. research report rr-48, Gas Processors Association, Tulsa, OK, 1982.
[62] T. Sako, T. Sugeta, N. Nakazawa, T. Obuko, M. Sato, T. Taguchi, and T. Hiaki. *J. Chem. Eng. Jpn.*, **24**, 449–454, 1991.
[63] R. W. Wiebe and V. L. Gaddy. *J. Am. Chem. Soc.*, **61**, 315–318, 1939.
[64] R. W. Wiebe and V. L. Gaddy. *J. Am. Chem. Soc.*, **63**, 475–477, 1941.
[65] J. Singh, J. G. Blencoe, and L. M. Anovitz, In steam, water, and hydrothermal systems, proceedings of the 13th international conference on the properties of water and steam; P. R. Tremaine, D. E. Irish, and P. V. Balakrishnan, eds., 2000.
[66] X. Chen, S. E. Gillespie, J. L. Oscarson, and R. M. Izatt. *J. Sol. Chem.*, **21**, 825–848, 1992.

LIST OF FIGURES

Figure 1. PT projection of the PTx surface for the water(1) + carbon dioxide(2) binary mixture. The circles correspond to the experimental vapour pressure of the pure water [40–48], the squares to the vapour pressure of the

pure carbon dioxide [49–54], the asterisks [55] and plusses [56] to critical data, and the triangles to the three-phase line data [9]. The continuous curves represents the SAFT-VR predictions for the vapour-pressures, the dashed curves the critical lines, and the long-dashed curve the three-phase line.

Figure 2. *Px* constant-temperature slices for the water(1) + carbon dioxide(2) binary mixture at 288.15 (a) and 348.15 K (b). The open circles correspond to the experimental VL and LL phase equilibria (data at 288.15 K is taken from references [57, 58] and data at 348.15 K from references [59–64]) and the continuous curves to the (VL and LL) phase envelopes. The dashed curve in part (a) indicates three-phase coexistence conditions and the solid circles the three coexistence phases at this temperature and pressure.

Figure 3. Excess volumes for the water(1) + carbon dioxide(2) binary mixture at 673.15 K and several pressures. The curves correspond to the theoretical predictions and the symbols to the experimental data taken from the literature [65] at different pressures: 9.94 MPa (circles and solid curve), 14.94 MPa (squares and dotted curve), 19.94 MPa (diamonds and dashed curves), and 24.94 MPa (triangles-up and long-dashed curve).

Figure 4. Excess enthalpies for the water(1) + carbon dioxide(2) binary mixture at 573.15 K and several pressures. The curves correspond to the theoretical predictions and the symbols to the experimental data taken from the literature [66] at different pressures: 11.0 MPa (circles and solid curve), 12.2 MPa (squares and dotted curve), and 13.8 MPa (diamonds and dashed curves). The thinner solid, dotted and dashed lines shown on the right hand represent the lines that connect the composition boundaries of the fluid-fluid two-phase regions at the corresponding pressures. The inset shows the H_2O-rich phase region in detail.

Table I: Optimised and re-scaled square-well intermolecular potential parameters for water [21] and carbon dioxide [19, 20].

Substance	m	σ(Å)	ϵ/k_B(K)	λ	ϵ^{HB}/k_B(K)	K^{HB}(Å^3)	σ_c(Å)	ϵ_c/k_B(K)	ϵ_c^{HB}/k_B(K)	K_c^{HB}(Å^3)
H_2O	1	3.033	300.4330	1.718250	1336.951	0.893687	3.469657	276.2362	1229.273	1.337913
CO_2	2	2.7864	179.27	1.515727	-	-	3.136386	168.8419	-	-

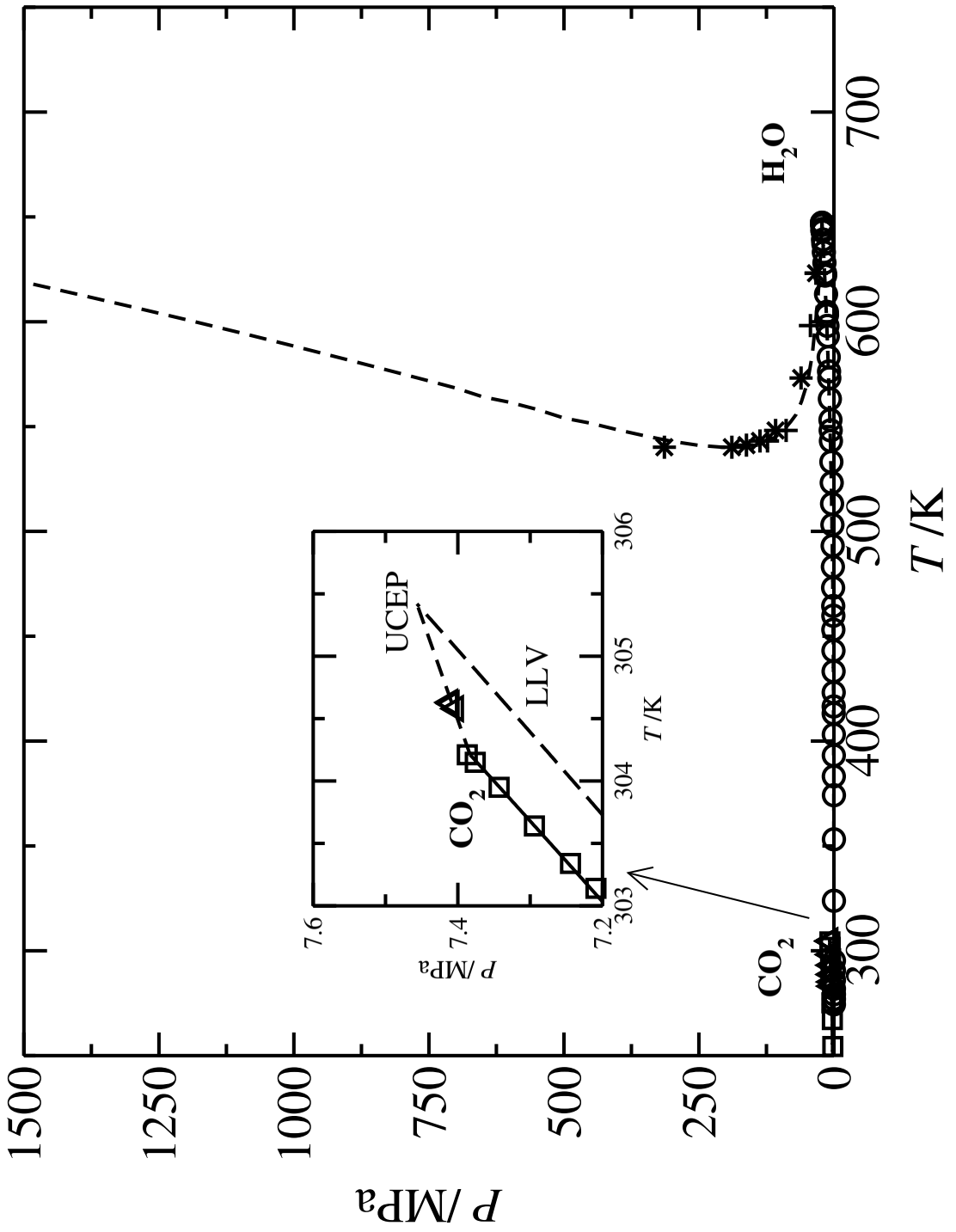

FIG. 1: dos Ramos, Blas and Galindo

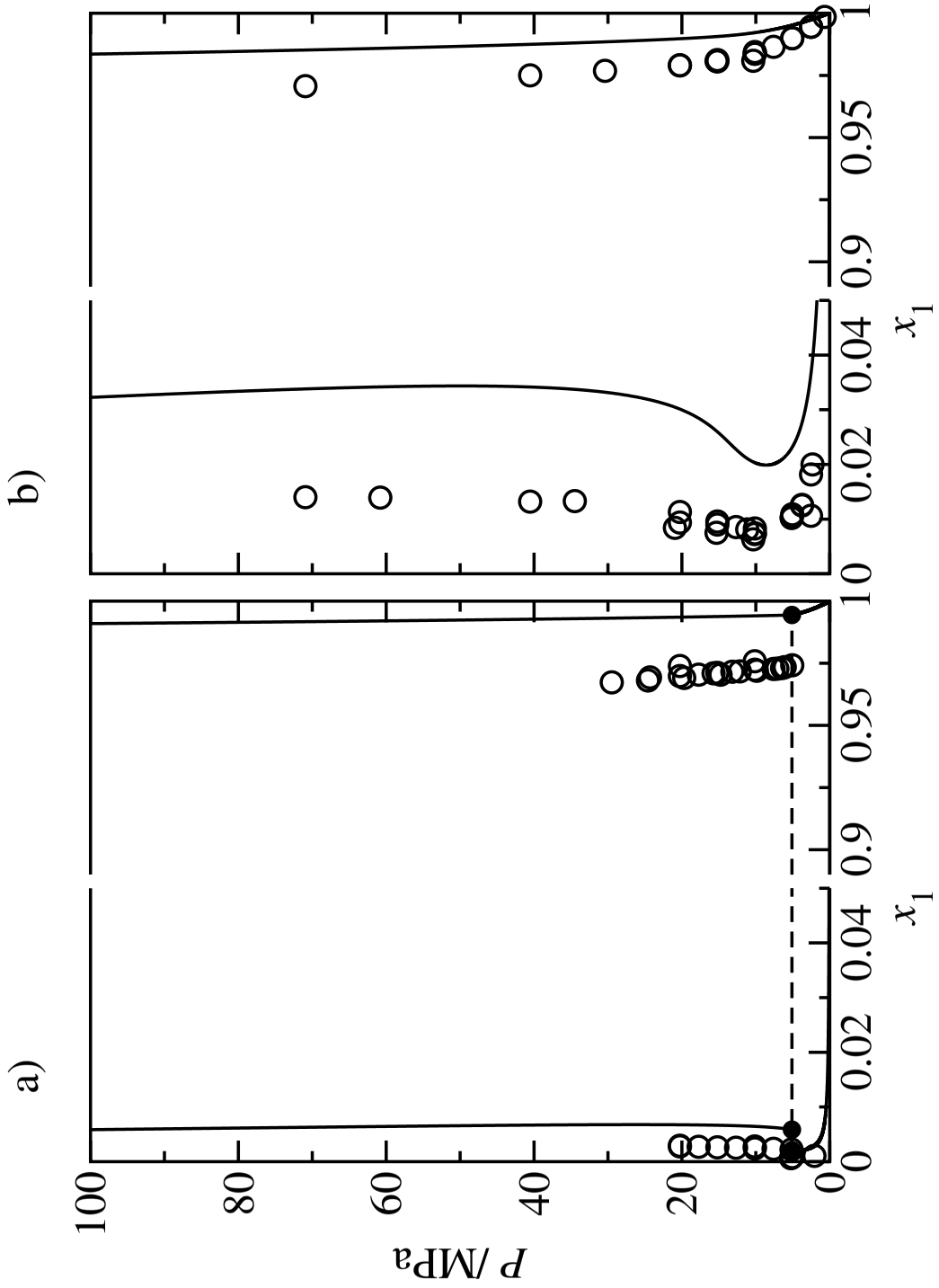

FIG. 2: dos Ramos, Blas and Galindo

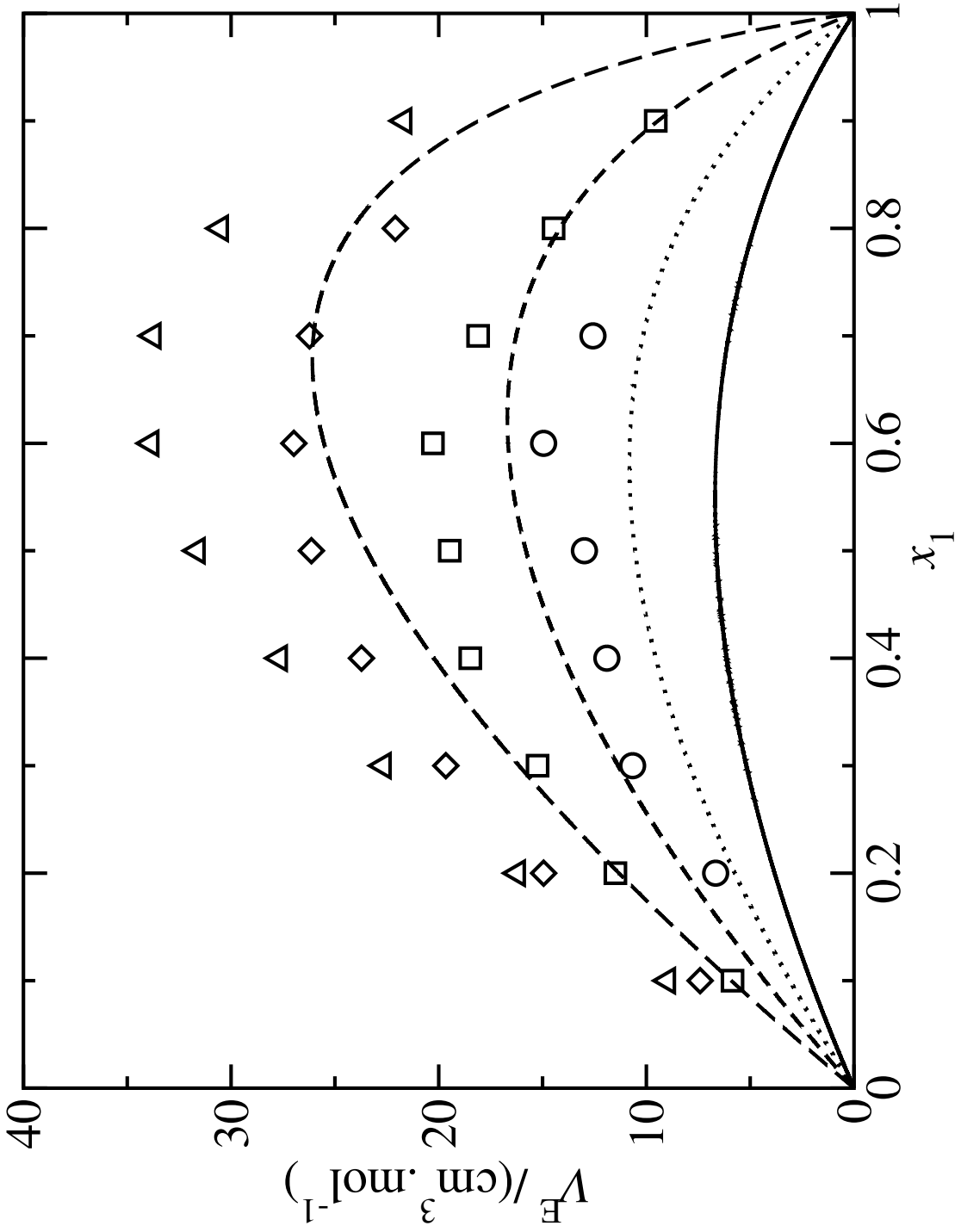

FIG. 3: dos Ramos, Blas and Galindo

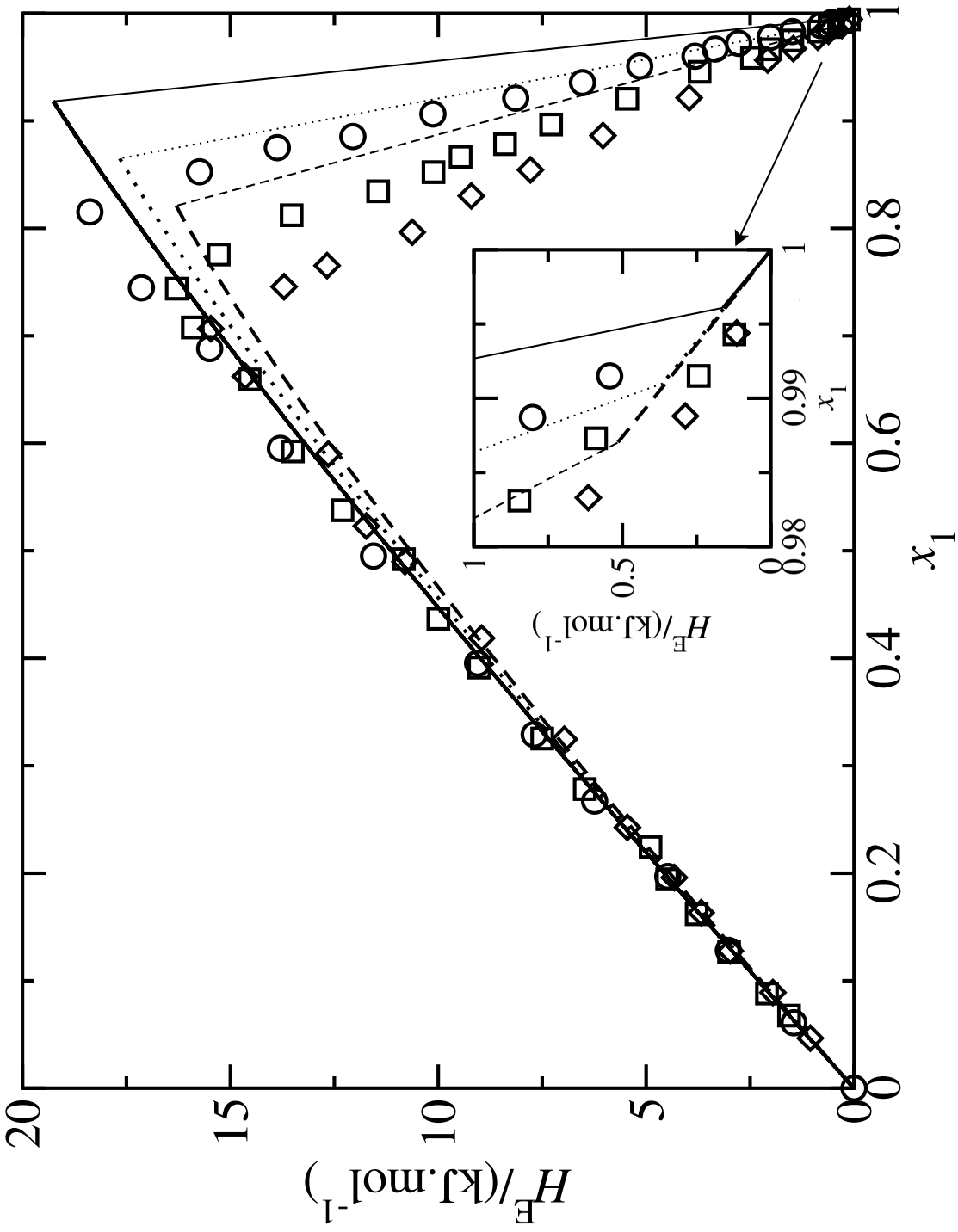

FIG. 4: dos Ramos, Blas and Galindo